Development of a small-scale spray-drying approach for amorphous solid dispersions (ASDs) screening in early drug development

Aymeric Ousset[a], Céline Bassand[b], Pierre-François Chavez[b], Joke Meeus[b], Florent Robin[b], Martin Alexander Schubert[b], Pascal Somville[b], Kalliopi Dodou[a]*

[a]*School of Pharmacy and Pharmaceutical Sciences, Faculty of Health Sciences and Wellbeing, University of Sunderland, Sunderland SR13SD, UK;* [b]*UCB Pharma S.A., Product Development, Braine l'Alleud B-1420, Belgium*

* Correspondence: kalliopi.dodou@sunderland.ac.uk; Tel.: +44-0191-515-2503

Development of a small-scale spray-drying approach for amorphous solid dispersions (ASDs) screening in early drug development

The present study details the development of a small-scale spray-drying approach for the routine screening of amorphous solid dispersions (ASDs). This strategy aims to overcome the limitations of standard screening methodologies like solvent casting and quench cooling to predict drug-polymer miscibility of spray-dried solid dispersions (SDSDs) and therefore to guarantee appropriate carrier and drug-loading (DL) selection. A DoE approach was conducted to optimize process conditions of **ProCept 4M8-TriX spray-drying** to maximize the yield from a 100 mg batch of Itraconazole/HPMCAS-LF and Itraconazole/Soluplus 40:60 (w/w). Optimized process parameters include: inlet temperature, pump speed, drying and atomizing airflows. Identified process conditions derived from the DoE analysis were further i) tested with Itraconazole, Naproxen and seven polymers, ii) adapted for small cyclone use, iii) downscaled to 20 mg batch production. Drug-polymer miscibility was systematically characterized using modulated differential scanning calorimetry (mDSC). Spray-drying was identified as a well-suited screening approach: mean yield of 10.1 to 40.6% and 51.1 to 81.0% were obtained for 20 and 100 mg ASD productions, respectively. Additionally, this work demonstrates the interest to move beyond conventional screening approaches and integrate spray-drying during screening phases so that a greater prediction accuracy in terms of SDSDs miscibility and performance can be obtained.

Keywords: amorphous solid dispersions; spray-dryer; design of experiments; screening; miscibility; solvent casting; quench cooling; polymers

Introduction

The increasing number of poorly water soluble compounds within drug pipelines poses problems in the drug development strategy of orally administrated formulations (Lipinski et al. 2012). The low solubility usually results in a limited dissolution rate and reduces the oral bioavailability of the drug. In this regard, amorphous solid dispersions (ASDs) can improve aqueous solubility and hence bioavailability of drugs (Vasconcelos

et al. 2007). This formulation strategy involves the dispersion of the amorphous drug particle within a polymeric matrix, achieved by a melt or a solvent method (Teja et al. 2013). From an industrial perspective, spray-drying is a well-known process used to convert solutions, suspensions and emulsions into powder at laboratory, pilot and commercial scale (Paudel et al. 2013).

In the past decades, laboratory spray-dryers have been routinely used in the pharmaceutical industry for the production of ASDs. Typically, this technique enables the production of milligram to gram scale batches and thereby is particularly suitable to support preclinical to early stage clinical activities (He and Ho 2015). In the current study, the ProCept laboratory spray-dryer was used due to its capability to work with a large range of feed solution volumes ranging from 0.5 mL to 24 liters/8 hours (ProCept 2014). Numerous studies have reported the optimization of spray-dried powder properties with a predominant focus on yield and particle size distribution (Amaro et al. 2011; Schmid et al. 2011; Lebrun et al. 2012).

However, the ability of laboratory spray-drying to provide reliable productions of solid dispersions during screening stage remains one major constraint (Ormes et al. 2013). It is well known that small batch size at the milligram scale results in a significant yield reduction of the spray-dried material. Few studies have considered the use of spray-drying for the production of solid dispersions at milligram scale (Chen et al. 2014; Gu et al. 2015). Nevertheless, the majority of the formulations investigated had generally limited drug-loading (DL) and were tested with a restricted number of drug and excipients. To the best of our knowledge, little has been published on the capability of spray-drying to be downscaled and adapted to the needs of screening phases of solid dispersions in early drug development. The use of spray-drying during small-scale ASDs screening remains limited in its current form and conventional

screening approaches, namely solvent casting and quench cooling are generally preferred (Dai et al. 2008; Parikh et al. 2015).

In a recent study, the authors demonstrated that standard screening methods like quench cooling and solvent casting performed at various evaporation rates cannot guarantee appropriate carrier and DL selection due to their limited accuracy to predict the phase behavior of spray-dried solid dispersions (SDSDs), consistently (Ousset et al. 2018). Despite conventional screening methodologies being the commonly used approach in the pharmaceutical industry, the influence of the preparation method on the properties and performance of ASDs generated during screening phase, and consequently on the carrier selection, should not be neglected. Given the importance to select appropriate polymer and DL in the early phase of drug development, there is an interest to move beyond traditional screening approaches in order to better anticipate SDSDs properties and performance. The novelty of this work consists of reconsidering the use of spray-drying in a small-scale approach and improving the prediction accuracy to determine the drug-polymer miscibility of SDSDs.

This work describes for the first time the development of a small-scale spray-drying approach for the screening of binary ASDs at preclinical stage and aims to define a generic method that can be used routinely in the pharmaceutical industry. In this regard, a particular attention has been given to develop a method in line with the screening requirements that: i) allows the testing of a large range of excipients and high DL, ii) can be applied on a large range of active drugs including low glass transition temperature (T_g) compounds, iii) produces solid dispersions at the milligram scale with optimized yield, short development time and limited amount of raw material, iv) respects the needs for subsequent analytical characterization of the screened

formulations, v) is representative and scalable with regard to formulation attributes and characteristics as well as process parameters and conditions.

First, a design of experiments (DoE) approach was conducted to identify robust processing conditions of drying airflow, inlet temperature, atomizing airflow and pump speed in order to optimize the yield of 100 mg productions of Itraconazole ASDs. The use of DoE is a well-established statistical method in compliance with quality by design (QbD) principles, and encouraged by the authorities (Q8(R2)-ICH) to provide a better understanding of the influence of formulation and process parameters on the quality attributes of the final product (Lebrun et al. 2012; Kauppinen et al. 2017). Second, the identified process conditions derived from the DoE approach were validated and tested with more polymers (listed in Table 1), an additional drug (Naproxen) and different DL. The process conditions were further adapted to the use of small cyclone, re-tested and downscaled to assess the spray-drying capability. The phase behavior of solid dispersions produced at small-scale ($\leq$ 100 mg) was analyzed using modulated DSC (mDSC) and X-ray powder diffraction (XRPD), and compared to samples prepared by spray-drying at larger scale (2.5 g), and by standard screening methodologies, namely solvent casting and quench cooling. **Finally, the performance of screened SDSDs of Itraconazole and Naproxen in terms of solubility enhancement and physical stability was also investigated.**

Materials and methods

Materials

Naproxen and Itraconazole were purchased from SRIS Pharmaceuticals (Hyderabad, India). Hydroxypropylmethylcellulose phthalate (HPMCP HP50) and hydroxypropylmethylcellulose acetate succinate fine grade (HPMCAS-LF) were

obtained from Shin-Etsu (Tokyo, Japan). Copolymer of N-vinyl-2-pyrrolidone and vinyl acetate (PVPVA) was obtained from Ashland (Covington, KY, USA) and polyvinylpyrrolidone (PVPK30) was purchased from VWR (Heverlee, Belgium). Copolymer of polyvinyl caprolactam-polyvinyl acetate-polyethylene glycol graft co-polymer (Soluplus) was donated by BASF (Ludwigshafen am Rhein, Germany). Copolymer of methacrylic acid and methyl methacrylate 1:1 (Eudragit L100) and copolymer of methacrylic acid and ethyl acrylate copolymer 1:1 (Eudragit L100-55) were donated by Evonik (Essen, Germany). The solvents used were of analytical or HPLC grade.

Methods

2.1 Generic method development

2.1.1 SDSD production

Spray-dried binary solid dispersions were prepared using the laboratory scale ProCept 4M8-TriX spray-dryer (Zelzate, Belgium). The feed solution was pumped to the nozzle via a peristaltic pump Watson Marlow 530S (Falmouth, Cornwall, UK). The process was operating with a length of two chambers and in the open loop configuration. Cyclone was systematically used to separate solid particles from drying gas airflow via centrifugal forces (Wang et al. 2006). Regarding this equipment, the supplier proposes cyclone in four different sizes (small, medium, large, extra-large) for optimal product recovery (ProCept 2014). Cyclone efficiency is directly impacted by the product characteristics e.g. particle size and density (Miller and Gil 2012). In this study, medium cyclone was initially used as it represents the best compromise approach to separate particles with a wide range of size and operates with a wide range of processing

conditions. In this regard, medium cyclone is particularly adapted to the DoE approach where variable process conditions are tested and therefore particles with different properties are generated. Subsequently, identified process conditions derived from the DoE approach were tested with small cyclone. Powder was collected into a 2 mL glass vial for the 100 mg productions and into a standard aluminium pan (TA Instruments, Leatherhead, UK) in the case of the 20 mg batch production. Powder collection was done via a customized 3D printed funnel ensuring sealing of the system and reducing material loss during powder handling. The collected powders were stored in a vacuum oven for 48 hours. Output process parameters such as the chamber outlet temperature and the pressure drop (ΔP) over the cyclone were monitored via the acquisition system interface.

2.1.2 DoE approach

Based on literature review and prior knowledge, a risk assessment was conducted regarding yield impact and the following process parameters and material attributes were identified: four process parameters (drying airflow, inlet temperature, atomizing airflow and pump speed) and one material attribute (polymer type) (Patel BB et al. 2015; Singh and Van den Mooter 2016). As seen in Table 2, each process factor was studied at three levels while the polymer type was included in the DoE as categorical factor (two levels). Intrinsic properties of polymers such as T_g and viscosity were covered via the polymer type factor. Additional key experimental factors such as nozzle orifice diameter, cooling airflow, cyclone size, solid content, DL, model drug and solvent were kept constant. The predefined values of each process and material input are listed on Table 3.

In this DoE, the batch size and the DL were fixed at 100 mg and 40% (w/w), respectively, which is assumed to be representative of the operating conditions during screening at preclinical stage (Ayad et al. 2013; Lohani et al. 2014). Itraconazole, a BCS class II compound known for its extremely low solubility in water (estimated at approximately 1 ng/mL) was selected as model drug (Engers et al. 2010). Preliminary tests (data not shown) prior to the DoE study were performed to evaluate the physico-chemical properties of seven polymers (cellulose, PVP, acrylate and miscellaneous polymers). **This selection of seven polymers is a typical range of carriers tested during screening phases. The use of enteric polymers during preclinical drug development is of particular interest so that the limited hydration of such polymers in acidic pH conditions is preventing the release of amorphous drug substance and is limiting the risk of recrystallization into the stomach. The absorption can be therefore maximized in intestinal fluids where polymer hydration occurs (Ueda et al. 2014).**

Analyses regarding T_g measurement and viscosity of polymer solution at various concentrations were conducted due to their potential impact on the yield of spray-dried material (Paudel et al. 2013). Based on this preliminary evaluation, Soluplus, a non-ionic and amphiphilic polymer with relatively low T_g (approximately 70°C) (Djuris et al. 2013) and HPMCAS-LF an enteric (pH 5.5) cellulosic derivative polymer known for its relatively high T_g (approximately 122°C) and viscosifying properties at high concentration (Ueda et al. 2014) were selected as they represented extreme properties among excipients of the studied domain.

A response surface methodology (RSM) design including four continuous factors (three levels) and one categorical factor (two levels) was developed using JMP 11 software (SAS, Cary, NC, USA). A total of 33 experiments including two repeated

experiments and three center points were performed (Appendix). The analysis of variance (ANOVA) was computed to determine the statistical significance of each input variable on the selected response (yield). The non-significant terms were removed from the statistical model to optimize it. Then, the desirability of the response was evaluated and factor values were identified at maximized yield desirability. Finally, two dimensional contour plots were represented to visualize the influence of input variables on the response (yield).

2.1.3 Yield calculation and specification

Yield was identified as the main quality attribute and was integrated as response in the model for optimization purpose. Yield is calculated as the ratio between the amount of particles collected and the total amount of solid dissolved in the feed solution. The yield value is expressed in percentage (%).

Yield specifications were defined depending on the production size: more than 50% for 100 mg productions and more than 10% for 20 mg productions. The specification limits would result in sufficient spray-dried material for subsequent analytical characterization typically required during ASDs screening.

2.1.4 Model validation

In order to assess the robustness of the model, production of a 100 mg ASD batch of Itraconazole/HPMCAS-LF and Itraconazole/Soluplus 40:60 (w/w) was performed in triplicate using identified operating conditions and medium cyclone. The average yield value was computed and compared to the 95% prediction interval provided by the model.

2.1.5 Model verification and adaptation to the small cyclone use

Subsequently, the identified operating conditions were further: i) tested with the production of solid dispersions of Itraconazole and Naproxen mixed with a set of seven polymers at a fixed DL of 40% (w/w) (the listed parameters detailed in Table 3 were kept constant), ii) adapted to the use of the small cyclone, iii) re-tested with the productions of solid dispersions of Itraconazole and Naproxen at 40% and 20% (w/w) DL using small cyclone. **Naproxen was selected due to its challenging properties regarding the manufacturing of low T_g compounds (approximately 6 °C). As amorphous forms exist in a rubbery state above their T_g, the stickiness of amorphous material to the wall of the column would reduce tremendously the yield value of the spray-dried material (Paterson et al. 2005).**

2.1.6 Downscaling

Optimized process conditions using small cyclone were further downscaled to ASD production of 20 mg. Production of solid dispersions of Itraconazole and Naproxen mixed with a set of seven polymers was performed. Each formulation was evaluated at a DL of 20% and 40% (w/w), respectively.

2.2 Alternative ASD screening methodologies

2.2.1 Solvent casting

Stock solutions of drug and polymer with a solid content of 50 mg/mL were prepared using a binary solvent mixture of DCM/EtOH 2:1 (v/v). The stock solutions were mixed in the appropriate volumetric ratio and a final volume of 5 mL was spread on a teflon plate (21 cm × 15 cm). A 15 cm diameter funnel (VWR, Heverlee, Belgium) was put on top of the casting solution and the solvent evaporation was performed at room temperature for 1 week. The film casted solid dispersions were then removed from the

teflon plate and were stored in a vacuum oven for 48 hours to remove residual solvent.

2.2.2 Quench cooling

Quench cooling screening was performed using a TA Instruments Q1000 DSC (TA Instruments, Leatherhead, UK). Casted samples were heated at a temperature of up to 20 °C higher than the last thermal event e.g. melting of the drug or the T_g of polymer to obtain a molten mixture. A fast cooling temperature of down to -50 °C was applied to prevent the drug recrystallization from the molten state. Lastly, the quench cooled samples were analyzed in mDSC.

2.3. Analytical methods

2.3.1 Modulated DSC

mDSC analyses were performed using TA Instruments Q1000 calorimeter (TA Instruments, Leatherhead, UK). The chamber was purged with a 50 mL/min flow rate of dry nitrogen. Indium was used for temperature and enthalpy calibration. The heat capacity calibration was performed at 96.9 °C using sapphire disks. About 2 – 4 mg of powder was analyzed in closed standard aluminium pans (TA Instruments, Leatherhead, UK). Samples were heated from 0 °C to 210 °C at 2 °C/min combined with a modulation of ± 1 °C and a period of 40 sec. The thermograms were collected and T_g was evaluated in the reverse heat flow signal using Universal Analysis 2000 software (TA Instruments, Leatherhead, UK).

2.3.2 X-ray powder diffraction

XRPD experiments were conducted on X Bruker AXS D8 Advance (Bruker, Karlsruhe, Germany). A few milligrams of powder were dropped on the center of a silicium

monocrystal holder. Samples were analyzed over the range 4.5 - 30° at a scan speed of 2.5 sec/step and a step size of 0.02°. The diffractograms were collected and processed using Eva DIFFRAC-SUITE software (Bruker, Karlsruhe, Germany). The integrated patterns represented the intensity as a function of 2θ.

2.3.3 Scanning electron microscopy

Scanning electron microscopy (SEM) observations were performed using the JEOL JSM-IT300 SEM (JEOL, Tokyo, Japan) to characterize the shape and morphology of the spray-dried particles. Powder was attached to conductive double-sided carbon adhesive tape mounted on an aluminium stud and coated with gold. The SEM instrument was operated in high vacuum mode at an accelerating voltage of 5 kV and at a working distance of 20.9 mm. The data treatment was carried out using JEOL IT300 Operation software (JEOL, Tokyo, Japan).

2.3.4 Dissolution tests

Dissolution profiles of screened SDSDs of Itraconazole were obtained at a target drug concentration of 1 mg/mL from a dissolution medium of 50 mM phosphate buffer (pH 6.5) containing 2% Vitamin E TPGS as surfactant. Dissolutions tests of screened SDSDs of Naproxen were performed in dissolution mediums consisting of i) simulated gastric fluid without pepsin (pH 1.2) containing 0.5% SDS and 2% HPMC at a drug concentration of 1 mg/mL, and of ii) 50 mM phosphate buffer (pH 6.5) containing 0.5% SDS and 2% HPMC at 5mg/mL. Dissolution tests were performed under non-sink conditions with respect to the crystalline drug. This would allow discriminating screened SDSDs on their potential to generate and maintain supersaturation (Sun et al. 2016). In this regard, target drug concentration was selected greater than the solubility of crystalline drug in the

chosen dissolution mediums. Accurate weight of 2.5 mg and 12.5 mg of SDSD (equivalent to 1 mg and 5 mg of drug, respectively) was distributed in 10 mL glass tube (VWR, Heverlee, Belgium). 1 mL of cited above dissolution medium was added to each tube. Temperature and magnetic stirring were maintained at 37°C and 350 rpm, respectively, using Thermo Mixer C unit (Eppendorf, Hamburg, Germany). During dissolution tests, samplings of 80 µL were withdrawn after 1, 5, 10, 15, 30, 60, 120 and 150 minutes. Samples were filtered on 0.45 µm ultrafree centrifugal filter units (Merck Millipore, Burlington, MA, USA) and centrifugated at 14000 rpm during 2 minutes. The filtrate was pipetted and then properly diluted in H_2O/ACN 1:1 (v/v). Itraconazole and Naproxen content was determined in HPLC coupled by UV detection at 260 and 272 nm, respectively. Similar protocol was applied to generate the dissolution profiles of crystalline Itraconazole and Naproxen in the tested dissolution mediums. All experiments were performed in triplicate.

2.3.5 Physical stability studies

Screened SDSDs of Itraconazole and Naproxen were stored at 40°C/75% RH and 25°C/60% RH for 5 weeks. Powder was analysed in XRPD at t_0, t_{2weeks} and t_{5weeks} in order to assess the potential of screened carriers to generate physically stable SDSDs under both stress and ambient conditions.

Results and discussion

DoE approach

The results obtained for the DoE are detailed in Appendix. Yield values ranging from 19.2% to 70.7% were obtained for the 100 mg batch production of

Itraconazole/HPMCAS-LF and Itraconazole/Soluplus 40:60 (w/w). The model obtained for the yield response was fitted using multiple linear regression. The statistical significance of the factors was evaluated based on the confidence level of 95%. The fitted model was adjusted by removing the non-significant factors while keeping the main effects. The p-value of the ANOVA (< 0.05) and the adjusted R-Squared value of 0.76 show that the response is described significantly by the optimized model (Figure 1). Moreover, the model does not present lack of fit (p-value > 0.05), demonstrating its suitability.

Based on DoE analysis and ANOVA results, seven factors including the main effects and the interaction terms were identified to have a significant influence on the response (p-values < 0.005). The main factors are ranked according to their impact on yield: atomizing air > HPMCAS-LF formulations > inlet temperature > drying airflow > interaction term between drying airflow and HPMCAS-LF formulations > pump speed > interaction term between the drying airflow and the inlet temperature. Interestingly, the type of polymer represented the second highest impacting effect on the yield. This reveals that the influence of this material attribute is as important as process parameters to understand yield variation of spray-dried material.

Figure 2 shows the conditions (factors values) identified for every polymer formulation if the yield desirability is maximized. Mean yield values of 58.6% and 75.6% were predicted for solid dispersions of Itraconazole/HPMCAS-LF and Itraconazole/Soluplus, respectively, at maximized desirability. The optimal values identified for the drying (0.45 m^3/min) and atomizing (1.5 bars) airflows as well as the inlet temperature (60 °C) were the same for both HPMCAS-LF and Soluplus ASDs.

The optimized value of the inlet temperature defined by the model was found at the lowest level of 60 °C. Indeed, the yield was negatively impacted by an increased

inlet temperature. Low inlet temperature reduces the outlet temperature at the bottom of the chamber and at the entry of the cyclone (Cal and Sollohub 2010). Under the optimized process parameter conditions, the outlet temperature was measured at around 40 °C; the outlet temperature is a good indicator of the product temperature to which the dried droplets are exposed (Maas et al. 2011; Paudel et al. 2013). High outlet temperature close or above the T_g of amorphous products favors material sticking on the glass walls and hence reduces significantly the yield (Paterson et al. 2005). Therefore, a low outlet temperature is particularly suitable for the production of ASDs with low T_g drug and/or polymer.

According to the model, drying and atomizing airflows were positively correlated to the yield (Figure 2). Interestingly, atomization airflow was found as the main effect impacting the response and was positively correlated to the yield variation. In addition, a value of 0.45 m^3/min of drying airflow was found to maximize the yield for both formulations. This observation is consistent with the theory of spray-drying: high drying airflow is reducing the residual moisture of the final product and improves the particle separation in the cyclone (Maury et al. 2005). The value of ΔP over the cyclone represents the cyclone efficiency to separate particles from the drying gas (Elsayed and Lacor 2011). The ΔP value is mostly influenced by the drying and the cooling airflows. A ΔP value of 51 mbar was measured during the tests with the optimized method. This value was in agreement with the supplier specification to ensure an optimal particle separation (ProCept 2014).

Yet, pump speed was found to have a limited influence on the yield; DoE analysis revealed that the pump speed was identified as the least significant factor among the main effect terms. Moreover, the pump speed was found to influence the yield in an opposite way depending on the used polymer. The pump speed has a slightly

negative effect on the yield of HPMCAS-LF ASDs but a slightly positive effect on the yield of Soluplus ASDs. This difference can be attributed to feed solution properties such as viscosity which is inherently impacted by the polymer type.

Yield distribution map was constructed as a function of pump speed with each other variable process parameter. This aims to determine the pump speed value that enables the production of ASDs with various polymers in the context of generic method development. Figure 3 displays the two dimensional contour plot results that represent yield map for productions of 100 mg ASD of Itraconazole/HPMCAS-LF and Itraconazole/Soluplus 40:60 (w/w). The contour plots showed that a low pump speed in combination with optimal process parameter for inlet temperature, drying and atomizing airflows (Table 4 for further details) led to a maximum yield. Consequently, the pump speed value was set at 1 g/min.

Furthermore, the fitted model was used to simulate the average yield of 5000 productions using optimized process parameters as described in Table 4. The simulations were computed and the results are reported in Figure 4. Based on these simulations, the model predicted a mean yield above the specification limits being in line with minimum quantities needed for further characterization. Regarding HPMCAS-LF formulations, the simulations predict a risk of 5.3% to obtain a yield lower than 50% which can be considered as an acceptable risk in the scope of the development of a generic method for preclinical screening of ASDs.

Model validation

Production of 100 mg ASD batches of Itraconazole/HPMCAS-LF and Itraconazole/Soluplus 40:60 (w/w) was performed in triplicate under optimized process conditions using medium cyclone. Mean yield values of 54.0% ± 8.4 and 56.6% ± 3.6 were experimentally obtained for solid dispersions of Itraconazole/HPMCAS-LF and

Itraconazole/Soluplus, respectively, while the prediction interval at 95 % provided by the model predicted a yield of 47.9 to 69.1% and of 61.9 to 83.7%, respectively. The prediction interval provided by the model overestimates the experimental results generated for the production of Soluplus ASDs. However, experimental yield results were found above the specification limits for both mixtures. The last observation confirms the selection of identified process conditions in line with the scope of the study.

One explanation to the differences obtained between predicted and experimental yield results is the lack of understanding of response by the fitted model. The adjusted R-Squared value of the model (0.76) attests that other parameters influencing the yield need to be taken into consideration to better explain the observed variability (Figure 1). Concentration effects and solvent choice have not been investigated in this study and would probably impact the response too (Paudel et al. 2013).

Model and/or process parameter verification

The suitability of the optimized manufacturing method was then evaluated by producing a 100 mg batch of Itraconazole and Naproxen ASDs using medium cyclone. Samples were prepared in triplicate at 40% (w/w) DL with a set of seven polymers listed in Table 1. Table 5 reports the average yield and standard deviation values experimentally obtained. Mean yield values ranging from 44.4 to 56.3% and 49.0 to 59.6% were obtained for Naproxen and Itraconazole ASDs, respectively.

Nevertheless, four Naproxen/polymer and one Itraconazole/polymer combinations did not reach the specification value of 50% as shown in Table 5. The latter observation suggests that the initial choice to select HPMCAS-LF and Soluplus (mainly based on their thermal and viscosity properties) as model carriers in the DoE design may have been too restricted and other material attributes may have been omitted

(density, surface tension). The identified process conditions in their current form are not fitting to these new drug/polymer combinations and to a large extent cannot be applied as screening procedure as the yield specification has not been reached consistently.

Adaptation to the small cyclone use and model and/or process parameter verification

The identified operating conditions were further adapted to the use of the small cyclone: the drying airflow was decreased to 0.3 m^3/min to ensure a similar outlet temperature and a similar pressure drop over the cyclone compared to the previous operating conditions with the medium cyclone. As the small cyclone can only operate in a restricted domain, lower drying airflow was applied to avoid pressure overload in the system. All other parameters listed in Table 3 were kept constant. Table 4 summarizes the operating conditions applied using small cyclone.

Productions of 100 mg batches of Itraconazole and Naproxen ASDs were repeated under these novel operating conditions. **SEM microphotographs of 40:60 (w/w) Itraconazole SDSDs collected from the small cyclone are displayed in Figure 5. Particles smaller than 10 µm were obtained and collected after processing. The spray-dried particles showed spherical shape with both smooth and shrinked surface (Figure 5 a-b) and shriveled surface (Figure 5 c-f). This morphological shape is typical for spray-dried material manufactured at low inlet temperature (Tonon et al. 2008). Moreover, the structural morphological differences between powder made with different carriers arise from the physical characteristics of the solid crust formed during solvent evaporation which is largely influenced by polymer type (Vicente et al. 2013).**

Yield values obtained for the productions of ASD 40:60 (w/w) are detailed in Figure 6. Under these conditions, all screened drug-polymer combinations resulted in a

yield of above 50%. The results obtained are mainly explained by the improved performance of the small cyclone to collect powder from drying air. In the present study, the highest selectivity of small cyclone is particularly adapted in the case of the identified process conditions derived from the DoE approach: where the combination of a high atomizing gas flow (1.5 bars) and a low pump speed (1 g/min) should theoretically favor the formation of small particle sizes. Application of high spray gas flow will produce smaller droplets and hence smaller particle. At a constant atomizing gas flow, a lower pump speed will decrease the droplet size and hence the particle size (Patel BB et al. 2015). In this regard and based on the supplier documentation, the small cyclone offers the most selective particle separation of up to 1.5 µm (ProCept 2014). This finding contrasts with previous studies where a large particle size correlates with a high yield (He and Ho 2015).

Figure 7 represents the yield improvement of ASDs produced using small cyclone compared to initial medium cyclone. The use of the small cyclone improved the yield of the 100 mg ASD batches for both drugs, significantly. The overall yield for ASDs of Naproxen was 51.0% with the medium cyclone and 65.9% with the small cyclone. Similarly, the overall yield of solid dispersions of Itraconazole was improved from 54.4% to 68.0% by reducing cyclone size. Despite a significant increase in yield compared to the medium cyclone, the yield improvement was found to depend on the nature of the dug - polymer combination (Figure 7). This finding confirms earlier observations and highlights the importance of material attributes and more specifically feed solution properties on the response. Yield improvement was lower for solid dispersions made with HPMCP HP50, HPMCAS-LF, Eudragit L100 and Eudragit L100-55. These polymers were found to have the most important viscosifying properties among the set of polymers investigated (data not shown). Feed solutions with

high viscosity will engender bigger particles (Davis et al. 2017), as a result the relative selectivity of the small cyclone compared to the medium size is probably be the least significant.

Figure 6 represents the results obtained for additional productions of Itraconazole and Naproxen ASD at 20% (w/w) under optimized process conditions using the small cyclone. Yield results obtained at 20% DL (w/w) were found above the specification limits, consistently. Comparable yields were obtained for most of the drug-polymer combinations with a DL of 20% and 40% (w/w) except for Itraconazole/PVPVA and Naproxen/Soluplus. In these particular cases, the yield was decreased from 40% to 20% (w/w) DL. The last observation contradicts the common assumption that reducing DL is expected to increase the yield of spray-dried material, theoretically. This is because the T_g value of ideal glass solution is function of the T_g of the pure components in the blend and of the system composition: a reduction in DL is increasing the mixing T_g due to higher polymer content (Teja et al. 2013).This assumption considers the fact that generally the T_g of the polymer is higher than the T_g of the drug (Table 1). This argument takes into account ideal glass solutions, only. In this regard, amorphous forms with high T_g are usually considered as suitable for spray-drying production due to the limited risk of stickiness on the glass wall (Paterson et al. 2005). Nevertheless, results obtained in the present study highlighted that the nature of the drug and its inherent properties such as T_g did not influence the yield. Mean yield of 20% and 40% (w/w) solid dispersions of Naproxen and Itraconazole was 64.1 ± 4.7% and 66.8 ± 5.6%, respectively. Consequently, the proposed method can be considered as a well-suited approach for the ASDs screening of low T_g drug such as Naproxen.

Downscaling

Downscaling trials were performed to assess the capability of spray-drying to operate at

minimum batch size while supporting the requirements for screening and analytical characterization. At this stage, a yield superior to 10% corresponding to 2 mg of ASD collected is sufficient to investigate the phase behavior and the solid state of screened formulations. As shown in Figure 8, optimized process conditions using the small cyclone were tested for 20 mg batch productions of Itraconazole and Naproxen ASD at 20 and 40% DL (w/w), respectively. Mean yield values above the specification limits were obtained for all screened drug-polymer mixtures under these operating conditions. The lowest yield, 18.2 ± 8.1% corresponding to an average mass of 3.6 ± 1.6 mg of ASD was obtained for Naproxen/PVPK30 40:60 (w/w), whereas, the highest yield, 30.1 ± 10.5%, corresponding to a mass of 6.0 ± 2.1 mg of ASD was found for Itraconazole/PVPK30 40:60 (w/w).

In general, the results obtained at 40% (w/w) DL for Itraconazole samples were slightly above the results found for Naproxen samples except for HPMCP HP50. Data obtained at a batch size of 20mg suggest, that the yield seems to depend on the nature of the drug and the involved polymer; for instance, the yield was positively impacted by a lower DL for Naproxen samples mixed with HPMCAS-LF, PVPVA and Soluplus. However, similar yields were obtained for other Naproxen ASDs at both DL. Likewise for ASDs containing Itraconazole, the DL did not impact the yield and no correlation between the yield and the DL was found at a 20 mg scale. As the spray-drying is running at lowest possible operating conditions, the differences that are expected are probably hindered by these extreme operating conditions. Additional downscaling trials with a batch size of 10 mg were performed (data not shown). However, the minimal yield of 2 mg was not achieved for all drug-polymer systems, consistently.

Drug-polymer miscibility characterization

Along with the development of a generic method adapted for the screening of small size

batches of ASD, the drug-polymer miscibility and the solid state of each SDSD produced at small and larger scale (20, 100 mg and 2.5 g) was characterized using mDSC and XRPD. Process and formulation parameters fixed during this DoE approach and listed in Table 3, were kept constant for the larger scale productions. Moreover, the following conditions of pump speed (6 g/min), inlet temperature (65 °C), drying airflow (0.35 m^3/min) and atomization airflow (1 bar) were used.

Figure 9 displays the mDSC thermograms of Itraconazole/PVPVA 40:60 (w/w) produced by spray-drying at various scales and prepared by standard screening methodologies, namely solvent casting and quench cooling. As seen in Figure 9, a glass solution, depicted by the presence of a single T_g in the reverse heat flow signal was obtained for the quench cooled sample. Residual crystallinity was detected in the film casted sample by the presence of the drug melting endotherm in both reverse and total heat flows. Additionally, the T_g of pure glassy Itraconazole with its inherent mesophase endotherms (Six et al. 2001) was found in the thermogram of film casted ASD and suggests the presence of a phase separated system (Six et al. 2002). Samples produced by spray-drying were identified as solid glass suspension. These samples are characterized by the presence of the T_g of the pure amorphous drug, the inherent mesophases of glassy Itraconazole and the T_g of the polymer. The absence of residual crystallinity was confirmed in the total heat flow signal of mDSC and by XRPD (data not shown). These results confirm that the above commonly used screening methods cannot predict the phase behavior of SDSDs.

The prediction accuracy of our small-scale spray-drying approach and conventional screening methodologies to determine the drug-polymer miscibility of SDSDs is compared Table 6, through the entire set of ASD productions giving a total of 28 samples. As seen in Table 6, the highest accuracy was obtained in the case of small-

scale spray-drying screening of 20 and 100 mg: these approaches allow for the drug-polymer miscibility prediction of 27/28 and 28/28 of SDSDs tested, respectively. One difference was obtained for Itraconazole/Soluplus 20:80 (w/w) produced at 20 mg and identified as a glass suspension while drug recrystallization occurred during analysis at 100 mg and 2.5 g. On the contrary, solvent casting and quench cooling did not provide a reliable insight into the prediction of the phase behavior of SDSDs over the set of tested drug-polymer combinations. Lower accuracy to predict the phase behavior of SDSDs than small-scale spray-drying approach was found for solvent casting and quench cooling with predictive ratio of 16/28 and 18/28 of SDSDs tested, respectively. In addition, the evaluation of thermograms (data not provided) showed that similar T_g value was obtained for samples produced by spray-drying at various scales. As T_g is known to provide insight into the stability and homogeneity of amorphous material, this demonstrated the superior ability of spray-drying screening compared to standard methodologies to anticipate the final properties and performance of SDSDs (Engers et al. 2010). This confirms the strategy developed in the current study in order to overcome the limitations of standard screening tests to predict SDSDs properties and performance in early phase of drug development.

Assessment of screened SDSDs potential: insight into physical stability and dissolution performance

Carrier performance with regard to the manufacture of glass solutions that improve drug solubility and that remain physically stable upon storage needs to be assessed during the screening phase (Chiang et al. 2012). In this regard, the performance of 100 mg batches of Itraconazole and Naproxen 40:60 (w/w) SDSDs have been investigated in terms of physical stability and dissolution performance.

The selected drug-polymer ratio is appropriate to reach the high doses to be tested during preclinical stage of drug development in the pharmaceutical industry (Lohani et al. 2014).

The XRPD patterns of 40:60 (w/w) SDSDs of Itraconazole are depicted in Figure 10. All screened drug-polymer systems were characterized by the presence of amorphous halo. The absence of peaks relative to crystalline drug in XRPD pattern confirms that all screened samples are manufactured in amorphous state after processing. However, as aforementioned in previous section, the evaluation of drug-polymer miscibility using mDSC confirms the presence of glass solution system with HPMCP HP50, HPMCAS-LF, Eudragit L100 and Eudragit L100-55 and the presence of phase separation with PVPVA and PVPK30, as seen in Table 6. Furthermore, glass solution followed by drug recrystallization during measurement was obtained in the case of Itraconazole/Soluplus system. Therefore, mDSC was proven to be a more sensitive technique to differentiate stable glass solutions from those which are prone to partial phase separation and drug recrystallization during the heating process (Baird and Taylor 2012).

The physical stability of Itraconazole-polymer combinations was investigated under stress (40°C/75% RH) and ambient (25°C/60% RH) storage conditions. Results are summarized in Table 7. Under standard storage conditions, all Itraconazole SDSDs maintained their inherent amorphous state during 5 weeks at 25°C/60% RH. XRPD pattern of Itraconazole SDSDs stored at 40°C/75% RH for 5 weeks are shown in Figure 10. Under stress conditions, Itraconazole systems made with HPMCP HP50, HPMCAS-LF, Eudragit L100 and Eudragit L100-55 were found to remain amorphous. However, drug recrystallization was confirmed for Itraconazole/Soluplus system after 2 weeks at 40°C/75% RH. This finding

corroborates the thermal signature of Itraconazole/Soluplus obtained in mDSC where drug recrystallization was recorded during analysis. Indeed, drug recrystallization during the heating procedure of mDSC is a sign of limited capacity of polymer to stabilize the amorphous drug and therefore can provide valuable insight into the physical stability of amorphous system (Duarte et al. 2015). As seen in Figure 10, the onset of drug recrystallization detected for solid dispersions of Itraconazole with PVPVA and PVPK30 stored 5 weeks under stress conditions confirms the fact that phase separated systems are more prone to recrystallization than glass solutions.

Figure 10 displays the XRPD pattern of 40:60 (w/w) SDSDs of Naproxen after manufacturing. Examination of XRPD patterns confirms that only ASDs made with PVPVA and PVPK30 maintained a complete amorphous state after processing. Evidence of drug residual crystallinity was observed for remaining SDSDs made with HPMC HP50, HPMCAS-LF, Soluplus, Eudragit L100 and Eudragit L100-55. This finding confirms drug-polymer miscibility as summarized in Table 6. In this regard, only Naproxen-polymer systems characterized in amorphous state *i.e.* PVPVA and PVPK30 ASDs were subjected to stability studies. Results from stability study are summarized in Table 7 and XRPD pattern of Naproxen ASDs stored at 40°C/75% RH during 5 weeks is depicted in Figure 10. Under both ambient and stress conditions, Naproxen/PVPVA and Naproxen/PVPK30 were found to maintain complete drug amorphous state up to 5 weeks, which is a good indicator of polymer potential to stabilize amorphous drug upon storage. This argument strengthens the selection of such carriers for Naproxen SDSD manufacturing. Storage of ASDs systems containing hygroscopic carriers such as PVPVA and PVPK30 should be ideally done under dried

conditions to reduce drug mobility and hence prevent drug recrystallization (Rumondor et al. 2009).

In parallel to stability studies, the dissolution performance of screened Itraconazole SDSDs was assessed at 37°C in dissolution medium at pH 6.5 containing surfactants. Dissolution profile of screened Itraconazole SDSDs and solubility improvement percentage compared to crystalline drug after 60 and 150 minutes are depicted in Figure 11. After 60 minutes, all screened ASDs allowed to generate supersaturation and improve drug solubility, significantly. Solubility improvement in the range of 5679-6931% was obtained and thus confirms the greater solubility of amorphous Itraconazole form compared to crystalline counterpart. After 150 minutes, only four ASDs made with HPMCAS-LF, Soluplus, Eudragit L100 and Eudragit L100-55 allowed to maintain supersaturation during dissolution tests. These dispersions systems display similar solubility improvement percentages between 60 and 150 minutes. However, recrystallization process during dissolution tests characterized by sudden drop in solubility value was recorded for ASDs containing HPMCP HP50, PVPVA and PVPK30. Indeed, such ASDs lost their potential in enhancing drug solubility. As an example, solubility improvement of Itraconazole/PVPK30 fell back to 263% after 150 minutes.

The obtained dissolution profile of screened Itraconazole SDSDs correlates well with their inherent solid state and drug-polymer miscibility characterization discussed in the previous section. Indeed, ASDs containing HPMCAS-LF, Eudragit L100 and Eudragit L100-55, previously identified as glass solutions, were able to generate and maintain supersaturation during the entire dissolution test. Furthermore, Itraconazole/Soluplus was also found to provide improved drug

solubility up to 150 minutes during the dissolution tests. However, as seen in Table 7, this system tends to recrystallize upon storage at 40°C/75% RH. In addition, dissolution tests (data not shown) performed in the case of Itraconazole/Soluplus stored during 2 weeks at 40°C/75% RH reveal that this ASD lost its potential in increasing drug solubility contrary to other glass solutions: solubility improvement of 5679/5347% and 1097/825% at 60/150 minutes were obtained for Itraconazole/Soluplus after manufacturing and after 2 weeks under stress conditions, respectively. As aforementioned, phase separation was observed during solid state characterization of SDSDs containing PVPVA and PVPK30. This translated well with their inherent dissolution profile where recrystallization process was observed during dissolution tests. This demonstrates the higher tendency of phase separated system to revert back to their crystalline form during both dissolution tests and physical stability (Huang and Dai 2014). Interestingly, Itraconazole/HPMCP HP50 was found to not maintain supersaturation during the length of dissolution test, despite this system was identified as physically stable amorphous glass solution under stress and ambient conditions. This finding suggests that the mechanism of polymer stabilization that occurs at solid state and during dissolution is different (Brouwers et al. 2009; Chauhan et al. 2013) which justified that both dissolution and physical stability performance of ASD should be addressed during screening phases. The selection of HPMCP HP50 as potential carrier for Itraconazole SDSD development would not be considered as it does not meet the key expectations of solid dispersion performance during screening phases.

Similarly, the potential of screened SDSDs of Naproxen to improve drug solubility was investigated. Because Naproxen is an acidic compound of which

solubility varies greatly depending on pH value, dissolutions tests have been performed in dissolution mediums representative to pH of both gastric and intestinal fluids (Chowhan 1978). First, solubility improvement results of screened SDSDs of Naproxen recorded after 60 and 150 minutes in dissolution medium at pH 6.5 containing surfactants, are depicted in Figure 12. Only three screened systems containing PVPVA, PVPK30 and Soluplus were found to generate and maintain supersaturation during dissolution test. On the contrary, SDSDs made with HPMCP HP50, HPMCAS-LF, Eudragit L100 and Eudragit L100-55 recrystallized in the fists seconds of dissolution tests (data not shown) which explains the fact that solubility was not improved even after 60 minutes. As seen in Table 6, the fact that residual crystallinity was observed for these specific Naproxen-polymer systems after processing translates well with their limited dissolution potential. Likewise, Naproxen/PVPVA and Naproxen/PVPK30, previously identified as glass solution were found to display the best dissolution performance with solubility improvement in the range of 50% after 150 minutes. Interestingly, Naproxen/Soluplus exhibited similar potential that ASDs containing PVPVA and PVPK30 in terms of solubility enhancement, despite the fact that complete amorphization was not achieved after processing as seen in Figure 10. In this context, Thakral *et al.* found that Camptothecin/Soluplus solid dispersion led to a 75-fold increase of drug solubility while incomplete amorphization was reported after processing (Thakral et al. 2012). Potential explanations may arise from the amphiphilic structure of Soluplus which has been demonstrated to solubilize drug and retard crystallization mechanisms through micellar formation (Shamma and Basha 2013; Patnaik 2016). Herein, Naproxen-Soluplus affinity would probably help in the stabilization of supersaturated solution generated by

dissolved amorphous drug fraction and prevent additional recrystallization process during dissolution test.

The potential of PVPVA, PVPK30 and Soluplus to improve Naproxen solubility was confirmed in gastric dissolution medium at pH 1.2 containing surfactants. Figure 13 displays the dissolution profile and solubility improvement percentage compared to crystalline drug after 60 and 150 minutes of such Naproxen SDSDs. All drug-polymer combinations were found to generate and maintain supersaturation during dissolution tests. Comparable solubility improvement percentages ranging from 203-257% were obtained among tested carriers after 60 minutes. Soluplus based solid dispersion was found to provide similar dissolution performance than identified glass solutions. Additional tests including biorelevant conditions and simulation of intestinal absorption would be needed to discriminate among screened systems (Linn et al. 2012; Puppolo et al. 2017). Despite this, PVPK30 and PVPVA were found to offer the best guarantee to achieve the manufacturing of physically stable amorphous system of Naproxen upon storage and providing solubility enhancement.

The results obtained in the present study prove that spray-drying can be adapted during the screening phases of ASDs and replaces existing screening methods. Productions of 100 mg of ASD under optimized operating conditions would provide enough material to ensure conventional preclinical screening activities (solid state characterization, dissolution tests, physical stability assessment). In parallel, downscaled trials allowed to assess the capability of spray-drying to run at lowest possible operating conditions while supporting the needs for screening and analytical characterization. In this regard, identified processing conditions allow the production of solid dispersion of 20 mg batch size that can be used as first step in carrier selection

with regards to solid state characterization of screened samples (mDSC, XRPD, polarized light microscopy…).

Otherwise, the proposed screening methodology focused on preclinical and small-scale manufacturing activities with a DL investigated up to 40% (w/w). Nevertheless, high DLs are commonly preferred in the final drug formulation regarding late clinical studies (Demuth et al. 2015; Patel S et al. 2017). In this regard, the proposed method would need to be further tested with higher DL to confirm that the amount of material collected is sufficient to cover the needs during screening phase. Additionally, a particular focus was placed on the ability of the proposed small-scale approach to predict the phase behavior of SDSDs which was found to provide valuable information regarding the physical stability and dissolution performance of screened SDSDs. Nevertheless, particle size distribution has not been particularly investigated in this study: it is assumed that particle size of powder generated at small-scale would not be representative for material produced by larger scale equipment where the nozzle geometry would generate larger particle size (Cal and Sollohub 2010).

In this study, DoE approach has been chosen to optimize process conditions of spray-dried material. As mentioned in the previous section, this approach has limitations such as the lack of understanding of response by the fitted model. However, when used in conjunction with mechanistic modelling can lead to a better understanding of the optimization process (Van Daele et al. 2017; Van Bockstal et al. 2018).

Conclusions

This study investigated the development of a generic screening method for ASD based on a small-scale spray-drying approach that respects the requirements of screening activities in the pharmaceutical industry. Optimized process conditions derived from DoE approach allowed the consistent production of ASD batches of 100 and 20 mg and

would ensured the production of sufficient material to support analytical characterization during screening phases. The proposed method was found particularly suitable for the testing of a large number of carriers and drugs, including low T_g compounds, and up to 40% (w/w) DL. In practical terms, this approach respects the scope of screening methodologies in particular the limited drug supply in early drug development: 4 to 8 mg and 20 to 40 mg of drug were needed per drug-polymer combination for the production of batch size of 20 mg and 100 mg, respectively. Although solvent casting and quench cooling approaches are known to operate in automated way and limit loss of product during screening phases, our proposed method constitutes a reliable alternative as it achieved the best trade-off regarding drug consumption, work flexibility and short processing time.

The main benefit of the implementation of spray-drying during screening phases is the improved prediction accuracy in terms of drug-polymer miscibility and performance of SDSDs: miscibility prediction accuracy of 27/28 and 28/28 of SDSDs tested was found for 20 and 100 mg SDSDs screening, respectively while lower accuracy was obtained for solvent casting (16/28) and quench cooling (18/28). In that respect, spray-drying screening was found to be representative and scalable with regards to process parameters as well as formulation attributes. This novel approach would allow to erase errors in polymer and DL selection during screening phases, ease the transfer from screening phase to laboratory batch production, and shorten delivery deadlines in the pharmaceutical industry. The outcome of the work demonstrates the interest to move beyond standard screening approaches and to consider the use of spray-drying in early phase of drug development so that a better prediction of SDSDs properties and performance can be achieved. **Indeed, this approach demonstrated**

that screened SDSDs of Itraconazole and Naproxen could be accurately discriminated in terms of physical stability and dissolution properties.

Acknowledgements, the authors would like to thank the PhD grant from the Product Development department, the technical support and assistance from the laboratory service and the solid state characterization group of UCB Pharma.

Declaration of interest, the authors report no conflict of interest.

References

Amaro MI, Tajber L, Corrigan OI, Healy AM. 2011. Optimisation of spray drying process conditions for sugar nanoporous microparticles (NPMPs) intended for inhalation. Int J Pharm. 421(1):99-109.

Ayad MH, Bonnet B, Quinton J, Leigh M, Poli SM. 2013. Amorphous solid dispersion successfully improved oral exposure of ADX71943 in support of toxicology studies. Drug Dev Ind Pharm. 39(9):1300-1305.

Baird JA, Taylor LS. 2012. Evaluation of amorphous solid dispersion properties using thermal analysis techniques. Adv Drug Deliv Rev. 64(5):396-421.

Brouwers J, Brewster ME, Augustijns P. 2009. Supersaturating drug delivery systems: the answer to solubility-limited oral bioavailability? J Pharm Sci. 98(8):2549-2572.

Cal K, Sollohub K. 2010. Spray Drying Technique. I: Hardware and Process Parameters. J Pharm Sci. 99(2):575-586.

Chauhan H, Hui-Gu C, Atef E. 2013. Correlating the behavior of polymers in solution as precipitation inhibitor to its amorphous stabilization ability in solid dispersions. J Pharm Sci. 102(6):1924-1935.

Chen XQ, Stefanski K, Shen H, Huang C, Caporuscio C, Yang W, Lam P, Su C, Gudmundsson O, Hageman M. 2014. Oral delivery of highly lipophilic poorly water-soluble drugs: spray-dried dispersions to improve oral absorption and enable high-dose toxicology studies of a P2Y1 antagonist. J Pharm Sci. 103(12):3924-3931.

Chiang PC, Ran Y, Chou KJ, Cui Y, Sambrone A, Chan C, Hart R. 2012. Evaluation of drug load and polymer by using a 96-well plate vacuum dry system for amorphous solid dispersion drug delivery. AAPS PharmSciTech. 13(2):713-722.

Chowhan ZT. 1978. pH-Solubility Profiles of Organic Carboxylic Acids and Their Salts. J Pharm Sci. 67(9):1257-1260.

Dai WG, Pollock-Dove C, Dong LC, Li S. 2008. Advanced screening assays to rapidly identify solubility-enhancing formulations: high-throughput, miniaturization and automation. Adv Drug Deliv Rev. 60(6):657-672.

Davis MT, Potter CB, Mohammadpour M, Albadarin AB, Walker GM. 2017. Design of spray dried ternary solid dispersions comprising itraconazole, soluplus and HPMCP: Effect of constituent compositions. Int J Pharm. 519(1-2):365-372.

Demuth B, Nagy ZK, Balogh A, Vigh T, Marosi G, Verreck G, Van Assche I, Brewster ME. 2015. Downstream processing of polymer-based amorphous solid dispersions to generate tablet formulations. Int J Pharm. 486(1-2):268-286.

Djuris J, Nikolakakis I, Ibric S, Djuric Z, Kachrimanis K. 2013. Preparation of carbamazepine-Soluplus solid dispersions by hot-melt extrusion, and prediction of drug-polymer miscibility by thermodynamic model fitting. Eur J Pharm Biopharm. 84(1):228-237.

Duarte I, Santos JL, Pinto JF, Temtem M. 2015. Screening methodologies for the development of spray-dried amorphous solid dispersions. Pharm Res. 32(1):222-237.

Elsayed K, Lacor C. 2011. The effect of cyclone inlet dimensions on the flow pattern and performance. Appl Math Model. 35(4):1952-1968.

Engers D, Teng J, Jimenez-Novoa J, Gent P, Hossack S, Campbell C, Thomson J, Ivanisevic I, Templeton A, Byrn S et al. 2010. A solid-state approach to enable early development compounds: selection and animal bioavailability studies of an itraconazole amorphous solid dispersion. J Pharm Sci. 99(9):3901-3922.

Gu B, Linehan B, Tseng YC. 2015. Optimization of the Buchi B-90 spray drying process using central composite design for preparation of solid dispersions. Int J Pharm. 491(1-2):208-217.

He Y, Ho C. 2015. Amorphous Solid Dispersions: Utilization and Challenges in Drug Discovery and Development. J Pharm Sci. 104(10):3237-3258.

Huang Y, Dai WG. 2014. Fundamental aspects of solid dispersion technology for poorly soluble drugs. Acta Pharm Sin B. 4(1):18-25.

Kauppinen A, Broekhuis J, Grasmeijer N, Tonnis W, Ketolainen J, Frijlink HW, Hinrichs WLJ. 2017. Efficient production of solid dispersions by spray drying solutions of high solid content using a 3-fluid nozzle. Eur J Pharm Biopharm. 123:50-58.

Lebrun P, Krier F, Mantanus J, Grohganz H, Yang M, Rozet E, Boulanger B, Evrard B, Rantanen J, Hubert P. 2012. Design space approach in the optimization of the spray-drying process. Eur J Pharm Biopharm. 80(1):226-234.

Linn M, Collnot EM, Djuric D, Hempel K, Fabian E, Kolter K, Lehr CM. 2012. Soluplus(R) as an effective absorption enhancer of poorly soluble drugs in vitro and in vivo. Eur J Pharm Sci. 45(3):336-343.

Lipinski CA, Lombardo F, Dominy BW, Feeney PJ. 2012. Experimental and computational approaches to estimate solubility and permeability in drug discovery and development settings. Adv Drug Deliv Rev. 64:4-17.

Lohani S, Cooper H, Jin X, Nissley BP, Manser K, Rakes LH, Cummings JJ, Fauty SE, Bak A. 2014. Physicochemical properties, form, and formulation selection strategy for a biopharmaceutical classification system class II preclinical drug candidate. J Pharm Sci. 103(10):3007-3021.

Maas SG, Schaldach G, Littringer EM, Mescher A, Griesser UJ, Braun DE, Walzel PE, Urbanetz NA. 2011. The impact of spray drying outlet temperature on the particle morphology of mannitol. Powder Technol. 213(1-3):27-35.

Maury M, Murphy K, Kumar S, Shi L, Lee G. 2005. Effects of process variables on the powder yield of spray-dried trehalose on a laboratory spray-dryer. Eur J Pharm Biopharm. 59(3):565-573.

Miller DA, Gil M. 2012. Chapter Spray-Drying Technology, Spray-Drying Technology. In: Williams III RO, Watts AB, Miller DA, editors. Formulating Poorly Water Soluble Drugs. New-York: Springer-Verlag; p. 363-442.

Ormes JD, Zhang D, Chen AM, Hou S, Krueger D, Nelson T, Templeton A. 2013. Design of experiments utilization to map the processing capabilities of a micro-spray dryer: particle design and throughput optimization in support of drug discovery. Pharm Dev Technol. 18(1):121-129.

Ousset A, Chavez PF, Meeus J, Robin F, Schubert MA, Somville P, Dodou K. 2018. Prediction of Phase Behavior of Spray-Dried Amorphous Solid Dispersions: Assessment of Thermodynamic Models, Standard Screening Methods and a

Novel Atomization Screening Device with Regard to Prediction Accuracy. Pharmaceutics. 10(1):29.

Parikh T, Gupta SS, Meena AK, Vitez I, Mahajan N, Serajuddin ATM. 2015. Application of film-casting technique to investigate drug-polymer miscibility in solid dispersion and hot-melt extrudate. J Pharm Sci. 104(7):2142-2152.

Patel BB, Patel JK, Chakraborty S, Shukla D. 2015. Revealing facts behind spray dried solid dispersion technology used for solubility enhancement. Saudi Pharm J. 23(4):352-365.

Patel S, Kou X, Hou HH, Huang YB, Strong JC, Zhang GGZ, Sun CC. 2017. Mechanical Properties and Tableting Behavior of Amorphous Solid Dispersions. J Pharm Sci. 106(1):217-223.

Paterson AHJ, Brooks GF, Bronlund JE, Foster KD. 2005. Development of stickiness in amorphous lactose at constant T−Tg levels. Int Dairy J. 15(5):513-519.

Patnaik S. 2016. Novel nanoformulations for enhanced oral bioavailability of some poorly water soluble non steroidal anti inflammatory drugs. Andhra Pradesh: Sri Sathya Sai Institute of Higher Learning.

Paudel A, Worku ZA, Meeus J, Guns S, Van den Mooter G. 2013. Manufacturing of solid dispersions of poorly water soluble drugs by spray drying: formulation and process considerations. Int J Pharm. 453(1):253-284.

ProCept. 2014. ProCept Information Brochure Spray dryer. Zelzate, Belgium: http://www.procept.be/spray-dryer-chiller.; [accessed].

Puppolo MM, Hughey JR, Dillon T, Storey D, Jansen-Varnum S. 2017. Biomimetic Dissolution: A Tool to Predict Amorphous Solid Dispersion Performance. AAPS PharmSciTech. 18(8):2841-2853.

Rumondor AC, Stanford LA, Taylor LS. 2009. Effects of polymer type and storage relative humidity on the kinetics of felodipine crystallization from amorphous solid dispersions. Pharm Res. 26(12):2599-2606.

Schmid K, Arpagaus C, Friess W. 2011. Evaluation of the Nano Spray Dryer B-90 for pharmaceutical applications. Pharm Dev Technol. 16(4):287-294.

Shamma RN, Basha M. 2013. Soluplus®: A novel polymeric solubilizer for optimization of Carvedilol solid dispersions: Formulation design and effect of method of preparation. Powder Technol. 237:406-414.

Singh A, Van den Mooter G. 2016. Spray drying formulation of amorphous solid dispersions. Adv Drug Deliv Rev. 100:27-50.

Six K, Leuner C, Dressman J, Verreck G, Peeters J, Blaton N, Augustijns P, Kinget R, Van den Mooter G. 2002. Thermal properties of Hot-stage extrudates of Itraconazole and Eudragit E100 Phase separation and polymorphism. J Therm Anal Calorim. 68:591-601.

Six K, Verreck G, Peeters J, Augustijns P, Kinget R, Van den Mooter G. 2001. Characterization of glassy itraconazole: a comparative study of its molecular mobility below Tg with that of structural analogues using MTDSC. Int J Pharm. 213:163-173.

Sun DD, Wen H, Taylor LS. 2016. Non-Sink Dissolution Conditions for Predicting Product Quality and In Vivo Performance of Supersaturating Drug Delivery Systems. J Pharm Sci. 105(9):2477-2488.

Teja SB, Patil SP, Shete G, Patel S, Bansal AK. 2013. Drug-excipient behavior in polymeric amorphous solid dispersions. J Excipients and Food Chem. 4(3):70-93.

Thakral NK, Ray AR, Bar-Shalom D, Eriksson AH, Majumdar DK. 2012. Soluplus--solubilized citrated camptothecin--a potential drug delivery strategy in colon cancer. AAPS PharmSciTech. 13(1):59-66.

Tonon RV, Brabet C, Hubinger MD. 2008. Influence of process conditions on the physicochemical properties of açai (Euterpe oleraceae Mart.) powder produced by spray drying. J Food Eng. 88(3):411-418.

Ueda K, Higashi K, Yamamoto K, Moribe K. 2014. The effect of HPMCAS functional groups on drug crystallization from the supersaturated state and dissolution improvement. Int J Pharm. 464(1-2):205-213.

Van Bockstal PJ, Mortier S, Corver J, Nopens I, Gernaey KV, De Beer T. 2018. Global Sensitivity Analysis as Good Modelling Practices tool for the identification of the most influential process parameters of the primary drying step during freeze-drying. Eur J Pharm Biopharm. 123:108-116.

Van Daele T, Gernaey KV, Ringborg RH, Börner T, Heintz S, Van Hauwermeiren D, Grey C, Krühne U, Adlercreutz P, Nopens I. 2017. Application of iterative robust model-based optimal experimental design for the calibration of biocatalytic models. Biotechnol Prog. 33(5):1278-1293.

Vasconcelos T, Sarmento B, Costa P. 2007. Solid dispersions as strategy to improve oral bioavailability of poor water soluble drugs. Drug Discov Today. 12(23-24):1068-1075.

Vicente J, Pinto J, Menezes J, Gaspar F. 2013. Fundamental analysis of particle formation in spray drying. Powder Technol. 247:1-7.

Wang B, Xu DL, Chu KW, Yu AB. 2006. Numerical study of gas–solid flow in a cyclone separator. Appl Math Model. 30(11):1326-1342.

Appendices

Appendix 1: Response surface DoE and yield results obtained for the 100 mg productions of ASD of Itraconazole at DL 40% (w/w).

Run	Drying airflow (m^3/min)	Inlet temperature (°C)	Pump speed (g/min)	Atomizing airflow (bars)	Polymers	Yield (%)
1	0.33	60	1	1	HPMCAS-LF	51.6
2	0.45	60	4.5	1	Soluplus	70.7
3	0.20	60	1	0.5	Soluplus	35.0
4	0.33	60	8	0.5	Soluplus	48.4
5	0.20	60	8	1.5	Soluplus	48.4
6	0.20	60	8	0.5	HPMCAS-LF	28.8
7	0.33	60	1	1.5	Soluplus	61.3
8	0.20	60	4.5	1.5	HPMCAS-LF	37.7
9	0.45	60	1	0.5	HPMCAS-LF	44.6
10	0.45	60	8	1.5	HPMCAS-LF	54.1
11	0.33	90	4.5	1	Soluplus	46.4
12	0.33	90	4.5	1	Soluplus	36.4
13	0.45	90	4.5	0.5	Soluplus	43.8
14	0.33	90	4.5	1	HPMCAS-LF	47.6
15	0.33	90	4.5	1	HPMCAS-LF	33.6
16	0.45	90	1	1	HPMCAS-LF	47.5
17	0.45	90	8	0.5	HPMCAS-LF	19.2
18	0.20	90	1	0.5	HPMCAS-LF	43.2
19	0.33	90	8	1.5	HPMCAS-LF	36.2
20	0.45	90	1	1.5	Soluplus	59.6
21	0.33	90	4.5	1	Soluplus	42.0
22	0.20	120	8	1	HPMCAS-LF	32.0
23	0.33	120	1	0.5	HPMCAS-LF	27.3
24	0.45	120	1	0.5	Soluplus	49.8
25	0.20	120	4.5	1.5	Soluplus	49.9
26	0.2	120	1	1.5	HPMCAS-LF	46.6
27	0.45	120	8	1	Soluplus	46.2
28	0.2	120	1	1	Soluplus	43.3
29	0.45	120	4.5	1.5	HPMCAS-LF	34.9
30	0.33	120	4.5	0.5	HPMCAS-LF	31.5
31	0.2	120	8	0.5	Soluplus	23.1
32	0.2	120	8	1	HPMCAS-LF	27.9
33	0.33	120	8	1.5	Soluplus	48.5

Tables

Table 1: Physicochemical properties of selected polymers.

Polymer	M_w (g/mol)	Dissolution pH	T_g (°C)
HPMCP HP50	78000	> 5.0	140
HPMCAS-LF	18167	> 5.5	122
PVPVA	57500	-	112
PVPK30	50000	-	162
Soluplus	115000	-	70
Eudragit L100	125000	> 6.0	192
Eudragit L100-55	320000	> 5.5	122

Table 2: Level values of process and formulation parameters included in the DoE.

Factors	Unit	Low level	Center level	High level
Drying airflow	m^3/min	0.2	0.33	0.45
Temperature inlet	°C	60	90	120
Atomizing airflow	bars	0.5	1	1.5
Pump speed	g/min	1	4.5	8
Polymer type	-	HPMCAS-LF	-	Soluplus

Table 3: List of process parameters, formulation attributes and process configuration kept constant in the DoE.

Factors	Unit	Value/attribute/configuration
Nozzle orifice diameter	mm	1.2
Cooling airflow	L/min	100
Cyclone size	-	Medium
Solid content	mg/mL	50
DL	% (w/w)	40
Drug	-	Itraconazole
Solvent	-	DCM/EtOH 2:1 (v/v)

Table 4: Optimized values of process parameters identified by the model and adapted for the small cyclone use.

Factors	Unit	Medium cyclone	Small cyclone
Drying airflow	m^3/min	0.45	0.3
Inlet temperature	°C	60	60
Atomizing airflow	bars	1.5	1.5
Pump speed	g/min	1	1

Table 5: Mean values of yield (%) and standard deviation (SD) (%) for solid dispersions of Itraconazole and Naproxen produced with the medium cyclone at a fixed DL of 40% (w/w).

Drug	DL	Cyclone	Polymers	HPMCP HP50	HPMCAS -LF	PVPVA	PVPK30	Soluplus	Eudragit L100	Eudragit L100-55
Itraconazole	40%	Medium	Yield (%)	54.4	54.0	53.4	49.0	56.6	59.6	53.5
			SD (%)	3.5	8.4	6.9	5.5	3.6	8.2	7.0
Naproxen	40%	Medium	Yield (%)	53.8	56.3	44.4	47.6	49.8	55.6	49.5
			SD (%)	2.7	2.7	4.1	4.4	2.2	2.6	3.9

Table 6: Miscibility characterization of ASDs produced by spray-drying at 2.5 g, 100 mg and 20 mg batch size and prepared by solvent casting and quench cooling for Itraconazole (a) and Naproxen (b) ASDs.

a) **Itraconazole ASDs**	DL (w/w)	**HPMCP HP50**	**HPMCAS -LF**	**PVPVA**	**PVPK30**	**Soluplus**	**Eudragit L100**	**Eudragit L100-55**
Spray-drying - 2.5 g	20%	GS	GS	GS	GS	DM/DR	GS	GS
	40%			PS	PS			
Small scale Spray-drying – 100 mg	20%	GS	GS	GS	GS	DM/DR	GS	GS
	40%			PS	PS			
Small scale Spray-drying – 20 mg	20%	GS	GS	GS	GS	PS	GS	GS
	40%			PS	PS	DM/DR		
Solvent casting	20%	GS	GS	DM/DR	DM/DR	DM/DR	GS	GS
	40%	PS	PS					
Quench cooling	20%	GS	GS	GS	GS	GS	GS	GS
	40%							
b) Naproxen ASDs	DL (w/w)	**HPMCP HP50**	**HPMCAS -LF**	**PVPVA**	**PVPK30**	**Soluplus**	**Eudragit L100**	**Eudragit L100-55**
Spray-drying - 2.5 g	20%	DM/DR	DM/DR	GS	GS	GS	GS	DM/DR
	40%					DM/DR	DM/DR	
Small scale Spray-drying – 100 mg	20%	DM/DR	DM/DR	GS	GS	GS	GS	DM/DR
	40%					DM/DR	DM/DR	
Small scale Spray-drying – 20 mg	20%	DM/DR	DM/DR	GS	GS	GS	GS	DM/DR
	40%					DM/DR	DM/DR	
Solvent casting	20%	DM/DR	GS	PS	GS	GS	DM/DR	DM/DR
	40%		DM/DR	DM/DR	DM/DR			
Quench cooling	20%	GS	GS	GS	GS	GS	GS	GS
	40%						DM/DR	DM/DR

Miscibility characterization examined by mDSC;

GS: glass solution, PS: Phase separation, DM/DR: drug melting/drug recrystallization

Table 7: Summary of stability results of 40:60 (w/w) solid dispersions of Itraconazole and Naproxen upon storage at 25°C/60% RH and 40°C/75% RH.

Drug	Carriers	DL (w/w)	25°C/60% RH		40°C/75%RH	
			2w	5w	2w	5w
Itraconazole	HPMCP HP50	40:60	N	N	N	N
	HPMCAS-LF	40:60	N	N	N	N
	PVPVA	40:60	N	N	N	Y
	PVPK30	40:60	N	N	N	Y
	Soluplus	40:60	N	N	Y	Y
	Eudragit L100	40:60	N	N	N	N
	Eudragit L100-55	40:60	N	N	N	N
Naproxen	PVPVA	40:60	N	N	N	N
	PVPK30	40:60	N	N	N	N

Residual crystallinity examined by XRPD; N: No crystalline signal, Y: crystalline signal

Figures

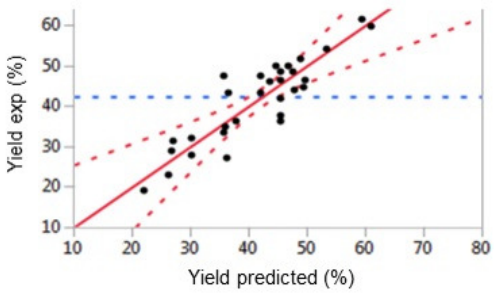

Lack of fit		
p-value Prob > F	0.7183	non-significant
ANOVA		
p-value Prob > F	<0.0001	significant
Summary of fit		
RSquare Adjusted	0.7592	
Root Mean Square Error	5.5226	

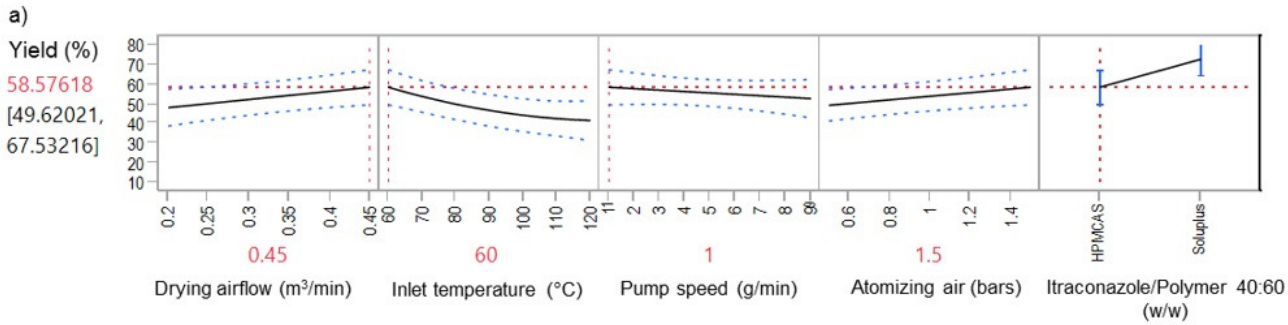

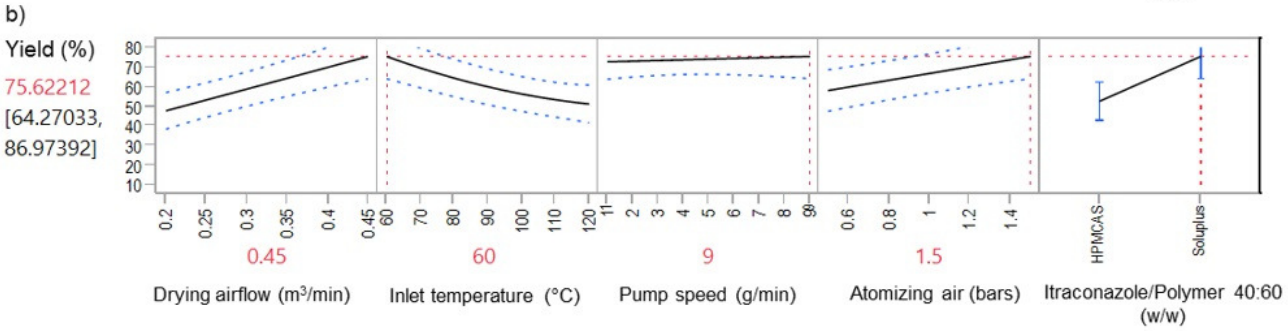

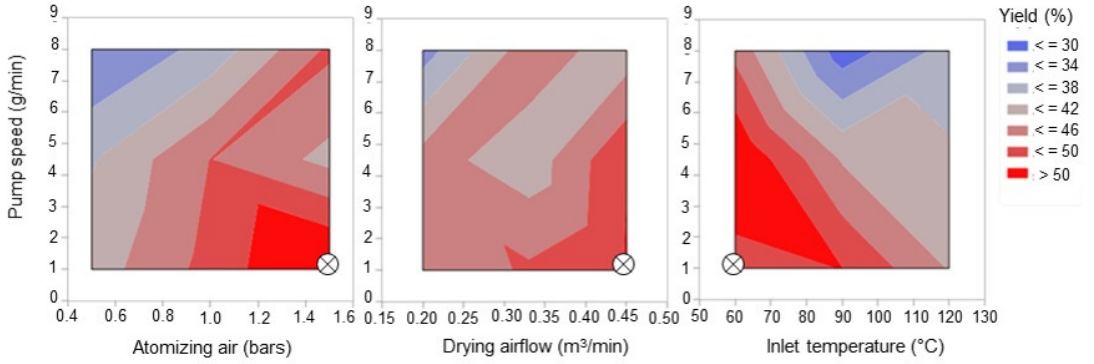

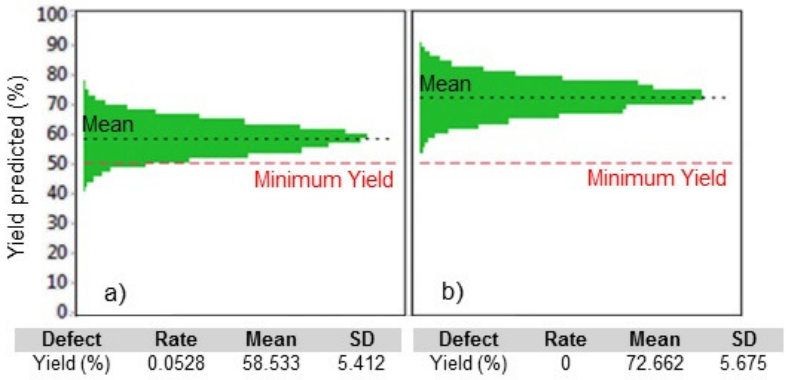

Defect	Rate	Mean	SD	Defect	Rate	Mean	SD
Yield (%)	0.0528	58.533	5.412	Yield (%)	0	72.662	5.675

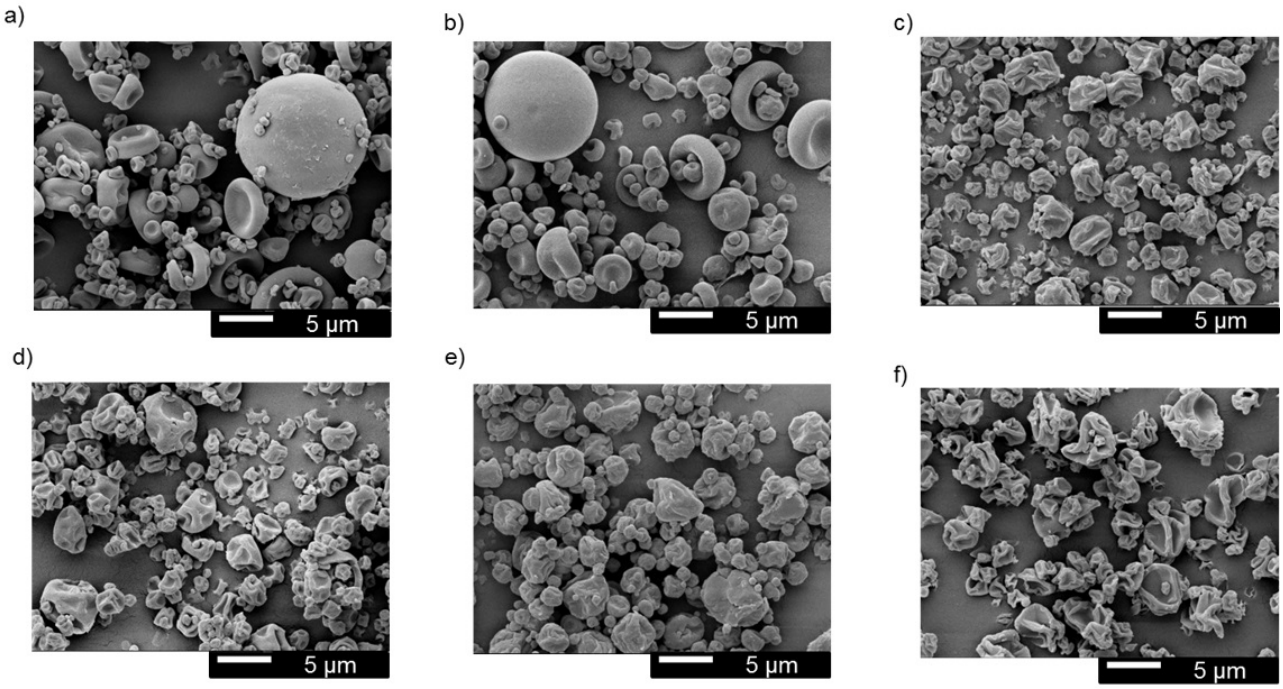

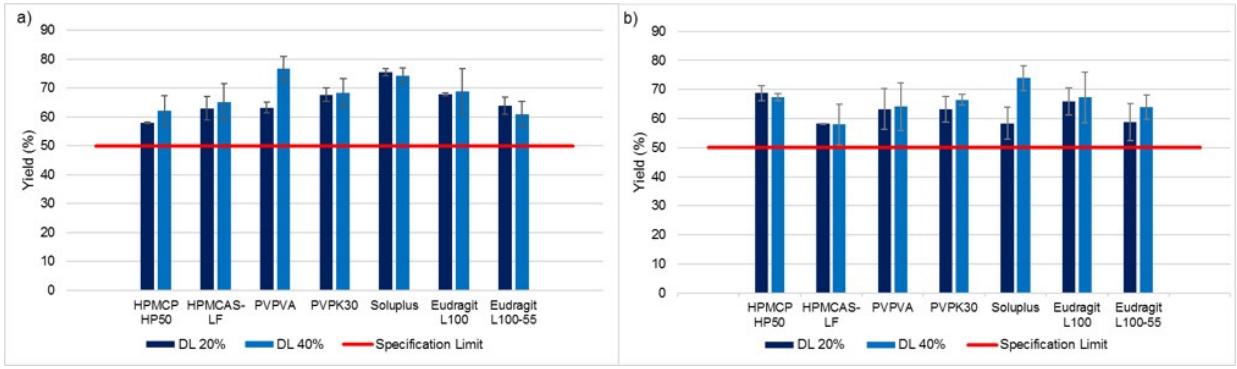
a)
b)
Yield (%)
HPMCP HP50
HPMCAS-LF
PVPVA
PVPK30
Soluplus
Eudragit L100
Eudragit L100-55
DL 20%
DL 40%
Specification Limit

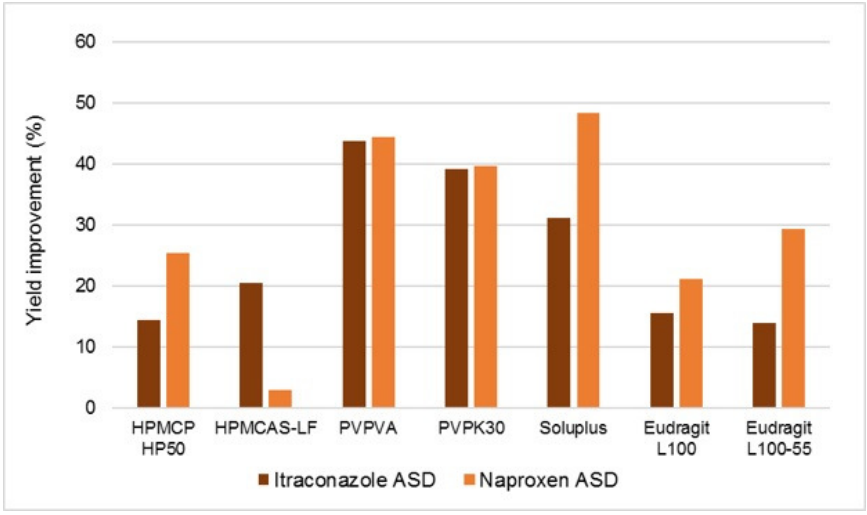
Yield improvement (%)
HPMCP HP50
HPMCAS-LF
PVPVA
PVPK30
Soluplus
Eudragit L100
Eudragit L100-55
Itraconazole ASD
Naproxen ASD

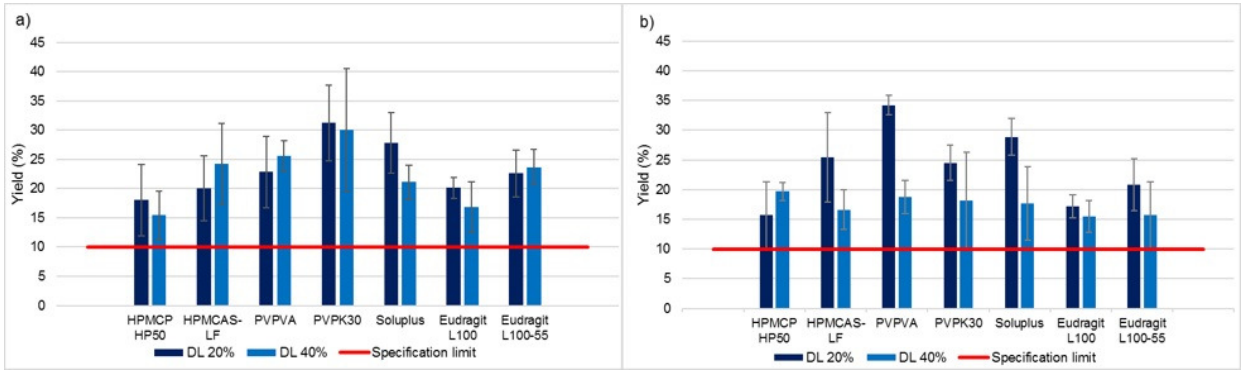
a)
b)
Yield (%)
HPMCP HP50
HPMCAS-LF
PVPVA
PVPK30
Soluplus
Eudragit L100
Eudragit L100-55
DL 20%
DL 40%
Specification limit

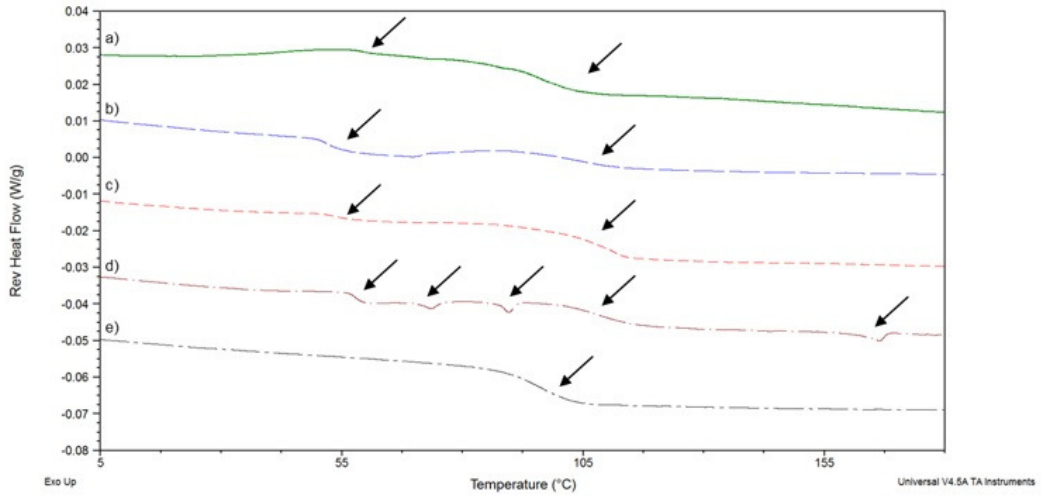
Rev Heat Flow (W/g)
Temperature (°C)
Exo Up
Universal V4.5A TA Instruments
a)
b)
c)
d)
e)

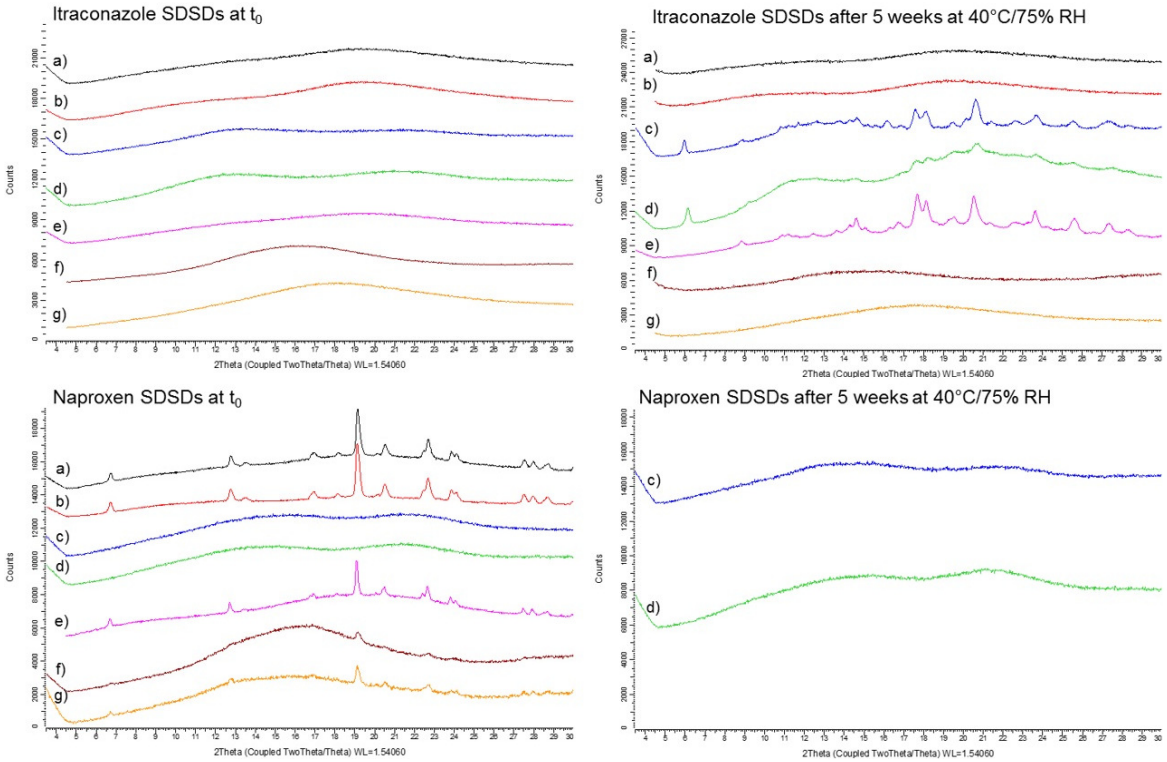
Itraconazole SDSDs at t0
Itraconazole SDSDs after 5 weeks at 40°C/75% RH
Naproxen SDSDs at t0
Naproxen SDSDs after 5 weeks at 40°C/75% RH
Counts
2Theta (Coupled TwoTheta/Theta) WL=1.54060

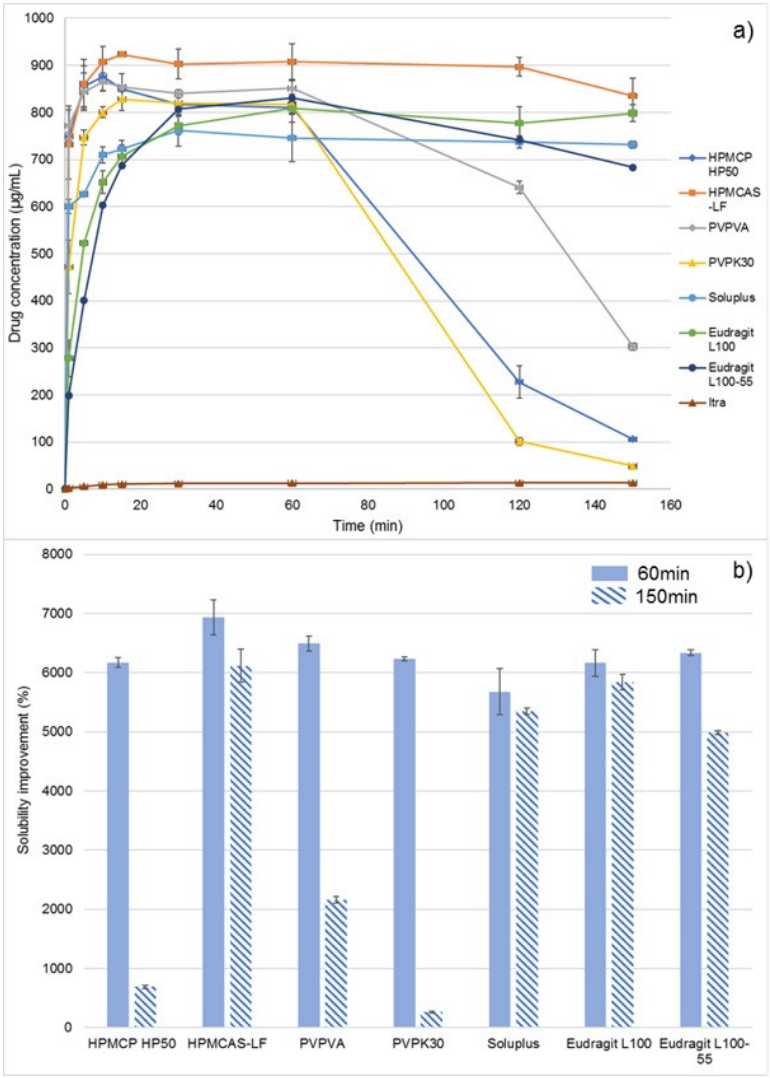
a)
Drug concentration (µg/mL)
Time (min)
HPMCP HP50
HPMCAS -LF
PVPVA
PVPK30
Soluplus
Eudragit L100
Eudragit L100-55
Itra
b)
60min
150min
Solubility improvement (%)
HPMCP HP50
HPMCAS-LF
PVPVA
PVPK30
Soluplus
Eudragit L100
Eudragit L100-55

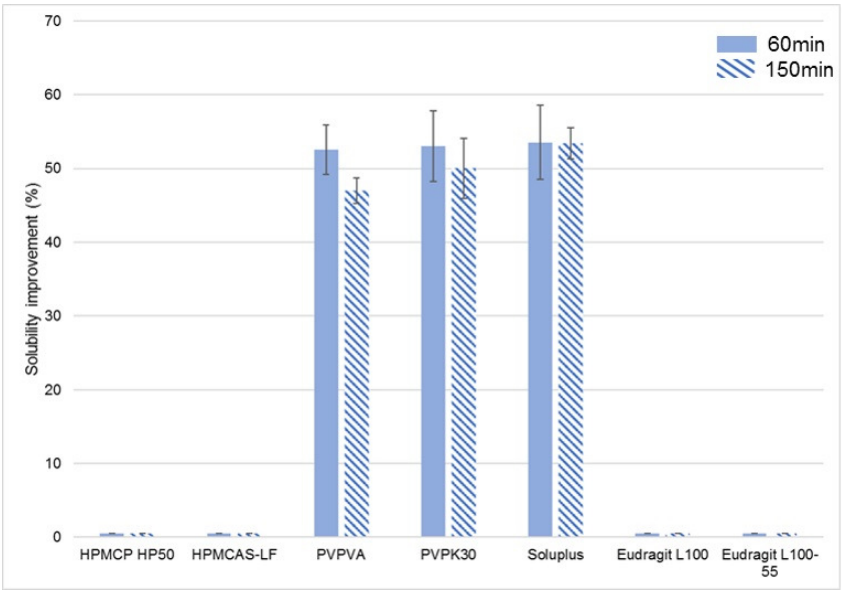
60min
150min
Solubility improvement (%)
HPMCP HP50
HPMCAS-LF
PVPVA
PVPK30
Soluplus
Eudragit L100
Eudragit L100-55

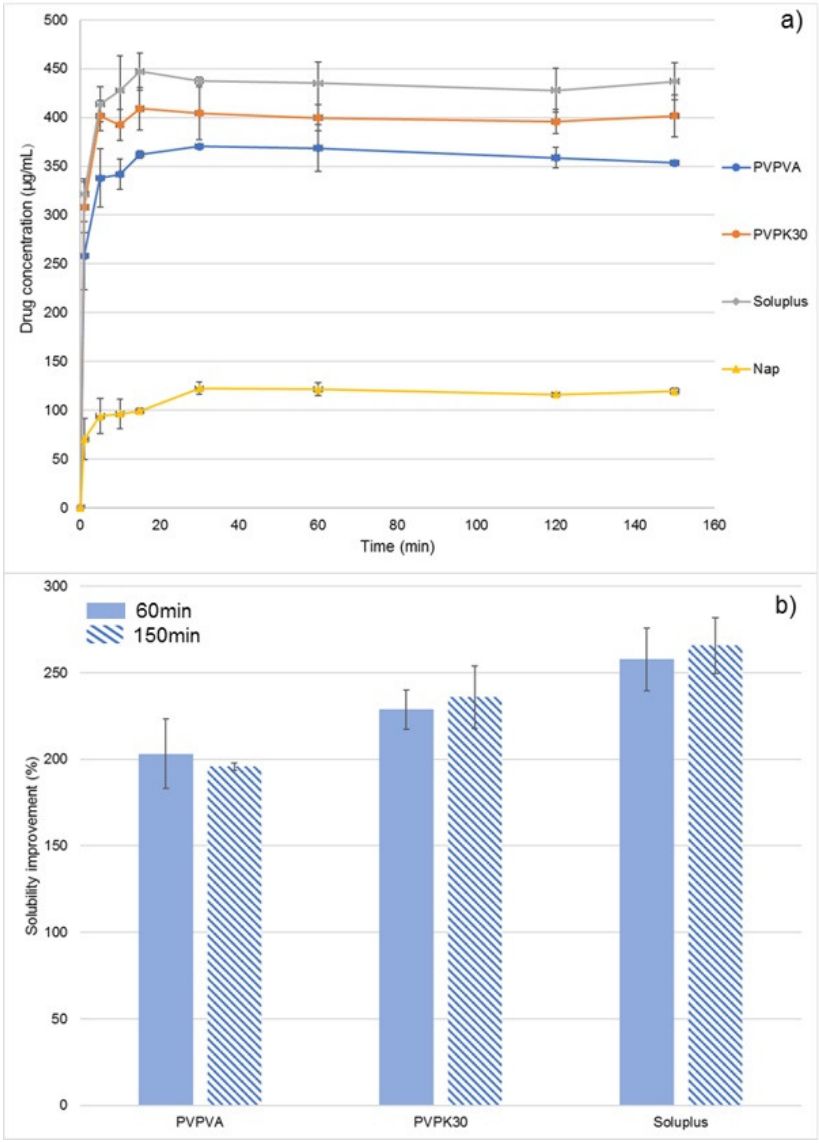
a)
Drug concentration (µg/mL)
Time (min)
PVPVA
PVPK30
Soluplus
Nap
b)
60min
150min
Solubility improvement (%)
PVPVA
PVPK30
Soluplus

Figure captions

Figure 1: Fit model analysis for yield prediction.

Figure 2: Maximized yield response for 100 mg production of spray-dried ASDs of Itraconazole mixed with HPMCAS-LF (A) and Soluplus (B) at 40% (w/w) DL. Confidence interval at 95% is represented in dash blue lines.

Figure 3: Distribution map of mean yield values as a function of pump speed with atomizing airflow, drying airflow and inlet temperature respectively, for overlapped 100 mg ASD productions of Itraconazole/HPMCAS and Itraconazole/Soluplus 40:60 (w/w) with optimized process conditions.

Figure 4: Yield distribution based on simulation of 5000 productions computed for the 40:60 (w/w) ASD of Itraconazole mixed with HPMCAS-LF (A) and Soluplus (B); under identified process conditions.

Figure 5: SEM microphotographs of 40:60 (w/w) Itraconazole SDSDs with: HPMCP HP50 (a), HPMCAS-LF (b), PVPVA (c), PVPK30 (d), Soluplus (e) and Eudragit L100 (f) collected from the small cyclone.

Figure 6: Average yield values (n=3) obtained for the 100 mg ASD productions of 20:80 and 40:60 (w/w) Itraconazole (a) and Naproxen (b) using the small cyclone. The minimum yield is represented by the solid red line at 50%.

Figure 7: Cyclone efficiency: yield improvement (%) for the 100 mg ASD productions of 40:60 (w/w) Itraconazole and Naproxen performed under optimized process parameters using small/medium cyclone.

Figure 8: Average yield values (n=3) obtained for the 20 mg ASD productions of 20:80 and 40:60 (w/w) Itraconazole (a) and Naproxen (b) using the small cyclone. The minimum yield is represented by the solid red line at 10%.

Figure 9: Reverse heat flow signals of Itraconazole/PVPVA 40:60 (w/w) produced by spray-drying for 2.5 g batch production (a), small-scale spray-drying approach for 20 mg (b) and 100 mg (c) batches production, quench cooling (d) and solvent casting (e).

The arrows indicated the presence of the T_g, the mesophases of glassy Itraconazole and the drug melting endotherm.

Figure 10: XRPD patterns of 40:60 SDSDs of Itraconazole and Naproxen just after processing and after 5 weeks under stress conditions at 40°C/75% RH, respectively with HPMCP HP50 (a), HPMCAS-LF (b), PVPVA (c), PVPK30 (d), Soluplus (e), Eudragit L100 (f) and Eudragit L100-55 (g).

Figure 11: Dissolutions profiles (a) and solubility improvement (%) (b) of screened 40:60 (w/w) Itraconazole SDSDs compared to crystalline drug after 60 and 150 minutes in 50 mM phosphate buffer (pH 6.5) containing 2% Vitamine E TPGS at a drug concentration of 1 mg/mL.

Figure 12: Solubility improvement (%) of screened 40:60 (w/w) Naproxen SDSDs compared to crystalline drug after 60 and 150 minutes in 50 mM phosphate buffer (pH 6.5) containing 0.5% SDS and 2% HPMC at a drug concentration of 5mg/mL.

Figure 13: Dissolutions profiles (a) and solubility improvement (%) (b) of screened 40:60 (w/w) Naproxen SDSDs compared to crystalline drug after 60 and 150 minutes in simulated gastric fluid (pH 1.2) containing 0.5% SDS and 2% HPMC at a drug concentration of 1 mg/mL.